



## Optimization of chemical and electrochemical parameters for the preparation of $n$ -type $\text{Bi}_2\text{Te}_{2.7}\text{Se}_{0.3}$ thin films by electrodeposition

S. MICHEL<sup>1</sup>, N. STEIN<sup>1</sup>, M. SCHNEIDER<sup>2</sup>, C. BOULANGER<sup>1,\*</sup> and J-M. LECUIRE<sup>1</sup>

<sup>1</sup>Laboratoire d'Electrochimie des Matériaux, UMR CNRS 7555

<sup>2</sup>Laboratoire de Chimie et Applications-E.A.No. 3471-Groupe Synthèses et Applications Organiques, Université de Metz, Ile du Saulcy, 57045 Metz Cedex 1, France

(\*author for correspondence, fax: +33 387 315 460, e-mail: boulang@sciences.univ-metz.fr)

Received 23 May 2002; accepted in revised form 22 October 2002

**Key words:** bismuth telluroselenide, electrodeposition, experimental design, X-ray diffraction

### Abstract

A  $2^{3-1}$  fractional factorial design comprising four runs and three centre points was applied in order to optimize the electrodeposition process to find a compound with the best stoichiometry leading to a  $\text{Bi}_2\text{Te}_{2.7}\text{Se}_{0.3}$  thin film suitable for thermoelectric applications. The key factors considered were the deposition potential, the percentage of bismuth and the percentage of selenium in the solution. The  $\text{Bi}^{\text{III}}$ ,  $\text{Se}^{\text{IV}}$ ,  $\text{Te}^{\text{IV}}$  electrolyte mixtures in 1 M  $\text{HNO}_3$  (pH 0), allowed deposition of ternary alloys to be achieved at room temperature on stainless steel substrates. The deposition mechanism was investigated by linear voltammetry. The films were characterized by microprobe analysis, X-ray diffraction, scanning electron microscopy and atomic force microscopy. The XRD patterns of the film show that the as-deposited are polycrystalline and isostructural to  $\text{Bi}_2\text{Te}_3$ . The SEM study shows that the film is covered by crystallites while the AFM image reveals a low level of roughness.

### 1. Introduction

Bismuth-based semiconductors are commonly used for thermoelectric devices such as thermoelectric generators [1, 2] and coolers [3] and for optical storage systems [4]. Bismuth telluride and its derivative selenide compounds are considered to be the best materials for use in thermoelectric refrigeration at room temperature [5, 6]. The current tendency towards miniaturization has increased the interest in microthermoelectric devices (sensors or generators). Electrodeposition also opens up opportunities for thin film microsystems. It has become well established that electrochemical deposition is a particularly attractive route for processing thin film semiconductor materials [7–9]. It offers the advantages of low synthesis temperature, low cost, large area deposition with minimum weight and thickness and high growth rates. Moreover, the synthesis experiments can be made in laboratory atmosphere, as opposed to growth physical techniques. Electrodeposition has been successfully applied to the production of bismuth telluride binaries [10–14]. The aim of this work was to produce a  $\text{Bi}_2\text{Te}_{2.7}\text{Se}_{0.3}$  alloy suitable for thermoelectric applications by exploring a potentiostatic process. The experimentation was performed using a  $2^{3-1}$  fractional factorial design. The accurate assessment of the factors' influence and the determination of the optimum were obtained from a reduced number of experiments.

### 2. Experimental details

#### 2.1. Voltammetric analytical study

Voltammetric experiments were carried out in a conventional three-electrode cell with a capacity of  $0.1 \text{ dm}^3$  at room temperature. The electrolyte solution was deaerated by argon bubbling for 30 min prior to the experiment and this atmosphere was kept constant during this experiment. The working electrode was a rotating platinum disc whose rotation rate was 625 rpm. All potentials were measured and are expressed relative to the aqueous KCl saturated calomel electrode (SCE). The counter electrode was a platinum wire. Voltammograms were obtained using a potentiostat/galvanostat Radiometer PGP 201 driven by a computer. Electrolytes were prepared in solution with deionized water. To ensure the stability and the solubility of bismuth (III) solutions, the selected solvent was 1 M aqueous  $\text{HNO}_3$ . The  $\text{Bi}^{\text{III}}$  and  $\text{Se}^{\text{IV}}$  solutions were obtained by dissolution of  $\text{Bi}(\text{NO}_3)_3 \cdot 5\text{H}_2\text{O}$  and  $\text{Na}_2\text{SeO}_3$  (analytical grade). The  $\text{Te}^{\text{IV}}$  solutions were prepared from the reaction of nitric acid on elemental tellurium (2N). The bismuth concentration was fixed at  $10^{-2} \text{ M}$  while the electrolyte concentrations varied from  $6.5 \times 10^{-3} \text{ M}$  to  $4.2 \times 10^{-3} \text{ M}$  for the tellurium and from  $1.4 \times 10^{-4}$  to  $3.8 \times 10^{-4} \text{ M}$  for the selenium.

## 2.2. Experimental design

To make the experimentation easier, a  $2^{3-1}$  fractional factorial design comprising two levels (noted +1, high and -1, low) and three centre points (noted 0) was used [15]. For purposes of analysis, it is convenient to list the runs in standard order, not in the order (randomized) in which they were made. The elemental analyses of the electrodeposited films removed from their supports were achieved using an electron probe microanalysis (Cameca SX 50) calibrated with  $\text{Bi}_2\text{Te}_3$  and  $\text{PbSe}$  standards. The tellurium, bismuth and selenium microanalyses were performed in ten different sections of the samples. The stoichiometry corresponded to the average of these ten values and was calculated with a total atom number assigned as 5. For each response, normal plots on probability paper were applied as a graphical tool for the detection of aberrant observations [16]. EPMA give analyses reproducible within  $\pm 1\%$ .

## 2.3. Deposition conditions

Stainless-steel discs were chosen as substrate for the preparation of  $\text{Bi}_2(\text{Te}_x\text{Se}_{1-x})_3$  films for potentiostatic deposition. Plates were mechanically polished with carborundum paper and with diamond paste (1  $\mu\text{m}$  size). After being polished, the electrodes were cleaned with distilled water followed by p.a grade methanol rinsing. The working electrodes were located horizontally in the bottom of a PTFE cell specially designed in our laboratory. A 2  $\text{cm}^2$  area was exposed for deposition. The cathodic polarisation was carried out at room temperature without stirring with a platinum disc counter electrode facing the working plate and with a saturated calomel electrode (SCE). The electrochemical cell, under an argon atmosphere, had an electrolyte volume of 0.1  $\text{dm}^3$  whose concentrations were similar to that of the voltammetric study.

## 2.4. Deposit characterizations

Samples were prepared after electrodeposition by thorough rinsing in three steps (nitric acid solution pH 1, deionized water and methanol) followed by drying in air. X-ray diffraction data were obtained with a curve detector (INEL,  $\text{CoK}_\alpha$  radiation). The morphology was studied using a scanning electron microscope (Philips XL 30) and an Atomic Force Microscopy (Topometrics Explorer).

## 3. Results and discussion

### 3.1. Voltammetry

The aim of the analytical study was to investigate the behaviour of the  $\text{Bi}^{3+}$ ,  $\text{HTeO}_2^+$ , and  $\text{Se}^{4+}$  electrolyte mixtures during linear voltammetry. Experiments in solution containing various  $|\text{Bi}|/(|\text{Se}| + |\text{Te}|)$  ratios rang-

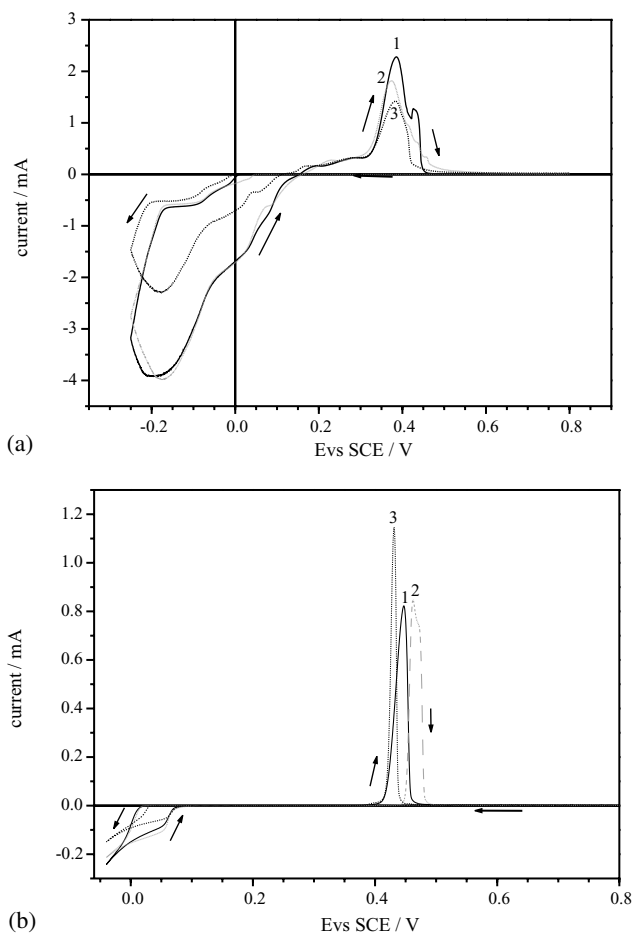
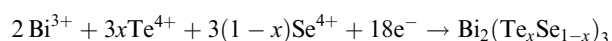


Fig. 1. Linear voltammogram in  $\text{HNO}_3$  1 M. Working electrode: platinum disc; surface area 3.14  $\text{mm}^2$ ; rotation rate 625 rpm; scan rate: 30  $\text{mV min}^{-1}$ . Curves: (1)  $10^{-2}$  M  $\text{Bi}^{3+}$  +  $6.5 \times 10^{-3}$  M  $\text{HTeO}_2^+$  +  $1.8 \times 10^{-4}$  M  $\text{Se}^{4+}$  (60 at. % Bi – 39 at. % Te – 1 at. % Se); (2)  $10^{-2}$  M  $\text{Bi}^{3+}$  +  $5 \times 10^{-3}$  M  $\text{HTeO}_2^+$  +  $3.9 \times 10^{-4}$  M  $\text{Se}^{4+}$  (65 at. % Bi – 32.5 at. % Te – 2.5 at. % Se); (3)  $10^{-2}$  M  $\text{Bi}^{3+}$  +  $4.2 \times 10^{-3}$  M  $\text{HTeO}_2^+$  +  $1.4 \times 10^{-4}$  M  $\text{Se}^{4+}$  (70 at. % Bi – 29 at. % Te – 1 at. % Se). Limit cathodic potential equal to  $-250$  mV (a) and  $-40$  mV (b).

ing from 1.5 to 2.33 were carried out. In Figure 1, linear voltammograms are shown for three different electrolytes containing: (1)  $10^{-2}$  M  $\text{Bi}^{3+}$  +  $6.5 \times 10^{-3}$  M  $\text{HTeO}_2^+$  +  $1.8 \times 10^{-4}$  M  $\text{Se}^{4+}$  (60 at. % Bi – 39 at. % Te – 1 at. % Se), (2)  $10^{-2}$  M  $\text{Bi}^{3+}$  +  $5 \times 10^{-3}$  M  $\text{HTeO}_2^+$  +  $3.9 \times 10^{-4}$  M  $\text{Se}^{4+}$  (65 at. % Bi – 32.5 at. % Te – 2.5 at. % Se), (3)  $10^{-2}$  M  $\text{Bi}^{3+}$  +  $4.2 \times 10^{-3}$  M  $\text{HTeO}_2^+$  +  $1.4 \times 10^{-4}$  M  $\text{Se}^{4+}$  (70 at. % Bi – 29 at. % Te – 1 at. % Se). A sweep rate of 30  $\text{mV min}^{-1}$  was used in these experiments. In a first step, the range of the potential exploration was conducted down to the proton reduction ( $-250$  mV) for the cathodic scans and up to the oxidation of electrodeposited material for the anodic ones (Figure 1(a)) with a main one situated at +400 mV. With increasing bismuth percentage in the solution, this main peak decreases while another peak situated at +100 mV is observed. The X-ray pattern of the compound obtained for a deposition potential equal to  $-250$  mV exhibits a Bi rich-phase. If the cathodic exploration is stopped at  $-40$  mV (Figure 1(b)), the

voltammetric curves are less complex and give one signal in the form of a reduction wave and one anodic peak which is well defined. Unlike the former deposition at  $-250$  mV, a reduction at  $-40$  mV leads to a single phase compound, isostructural with  $\text{Bi}_2\text{Te}_3$  compounds. Further studies were carried out with a cathodic stop at 0,  $-75$  or  $-110$  mV. The general shape of  $i = f(E)$  curve is very similar to that exhibited for a stop at  $-40$  mV. So, the voltammetric curves suggest that a deposition carried out at less cathodic potentials is able to induce a monophasic ternary alloy electroformation according to the following reaction:



### 3.2. Preparation of $\text{Bi}_2(\text{Te}_x\text{Se}_{1-x})_3$ films

In general, experiments are performed to measure the effects of one or more variables on one or more responses, and to find the set of variable combinations that gives the best result. Such an optimization process can be performed in several ways even though experimental design has become a rather widely used optimization tool thanks to its ease of use and the effectiveness of the method [17–19].

Experimental design follows a sequential approach, information gained in a first stage is then used to decide which factors should be maintained and studied in later stages. By so doing, as the study progresses, it is possible to reduce the size of the problem towards a smaller number of factors and to adjust their variation range to a more promising region that can be explored more thoroughly.

Table 1. Coded and uncoded levels of the three variables

Factors	Low Level (-1)	Mid Level (0)	High Level (+1)
$X_1$ : Potential vs SCE/mV	-125	-90	-55
$X_2$ : Atomic percentage of bismuth in the solution	60	65	70
$X_3$ : Atomic percentage of selenium in the solution	1	2.5	4

Preliminary studies carried out on the electrodeposition of binary or ternary alloys showed that the composition of alloys was influenced by chemical (electrolyte composition, in particular the  $|\text{Bi}|/(|\text{Se}| + |\text{Te}|)$  ratios) and electrochemical (potential) parameters. In this case, three parameters which could affect the response were identified: the deposition potential, the percentage of bismuth and the percentage of selenium in the solution (Table 1). The stoichiometry of each element was the response to be optimized in order to obtain a compound with the best stoichiometry  $\text{Bi}_2\text{-Te}_{2.7}\text{Se}_{0.3}$ .

A  $2^{3-1}$  fractional factorial design comprising 4 runs was chosen. As the (12) column to accommodate factor 3 was used, the equivalence  $3 = (12)$  was obtained (Table 2). This is called a resolution III design. It does not confound the main effects with one another but does confound the main effects with the two factor interactions. If the various linear contrasts are denoted by  $l_1, l_2$  and  $l_3$ ,  $l_1$  provides an estimate, not merely of the main effect of 1 nor of the (23)-interaction, but of the sum of these, that is,  $l_1 = 1 + (23)$ . Sometimes the results from a highly fractionated design can be ambiguous. In such a case it may be advisable to run a second fraction  $3 = -(12)$  which will resolve the uncertainties created by the first. Moreover, three experiments (runs 1,4,7 Table 2) were carried out at the centre of the design where all coded levels were zero and corresponded to the following uncoded levels: deposition potential equal to  $-90$  mV, 65 at. % of bismuth and 2.5 at. % selenium in the solution. These three experiments afforded the reproducibility of experiments, an estimate of the experimental error and the opportunity to check the validity of the model.

After electrodeposition, the stoichiometry of the ternary alloys is analysed for films removed from the support (Table 2). Several features can be observed. First, none of the seven runs obtains the desired stoichiometry. Secondly, an electrolyte containing 4 at. % Se is necessary to obtain a selenium stoichiometry close to or higher than 0.3 (runs 2 and 6). Thirdly, a deposition potential equal to  $-55$  mV is favourable to approach not only a tellurium content in the compound of to 2.7 but also a bismuth content of to 2 (runs 3 and 6).

Table 2. A  $2^{3-1}$  fractional factorial design in coded and uncoded units with responses  $y_{\text{Se}}$ ,  $y_{\text{Te}}$  and  $y_{\text{Bi}}$

Run	Experimental matrix			Experimental factors			Stoichiometry		
	$X_1$ (1)	$X_2$ (2)	$X_3$ (12)	$E$ vs SCE / mV	at. % Bi	at. % Se	$y_{\text{Se}}$	$y_{\text{Te}}$	$y_{\text{Bi}}$
1	0	0	0	-90	65	2.5	0.237	2.421	2.342
2	-	-	+	-125	60	<b>4</b>	<b>0.294</b>	2.191	2.515
3	+	-	-	<b>-55</b>	60	1	0.130	<b>2.635</b>	2.235
4	0	0	0	-90	65	2.5	0.196	2.351	2.453
5	-	+	-	-125	70	1	0.089	2.232	2.679
6	+	+	+	<b>-55</b>	70	<b>4</b>	<b>0.428</b>	2.448	<b>2.124</b>
7	0	0	0	-90	65	2.5	0.194	2.257	2.549

Table 3. Calculated effects and confidence interval for the  $2^{3-1}$  fractional factorial design

	Estimate $\pm$ 95% confidence limits		
	Selenium	Bismuth	Tellurium
Average	0.235 $\pm$ 0.012	2.388 $\pm$ 0.036	2.376 $\pm$ 0.033
$l_1 = 1 + (23)$	0.088 $\pm$ 0.025	-0.418 $\pm$ 0.073	0.330 $\pm$ 0.065
$l_2 = 2 + (13)$	0.047 $\pm$ 0.025	0.027 $\pm$ 0.073	-0.073 $\pm$ 0.065
$l_3 = 3 + (12)$	0.252 $\pm$ 0.025	-0.138 $\pm$ 0.073	-0.113 $\pm$ 0.065
Average of centre points	0.206 $\pm$ 0.009	2.461 $\pm$ 0.031	2.333 $\pm$ 0.0250

In view of the repeatability of these measures, the confidence interval can be assessed. It was calculated starting from the standard error of effects and Student's  $t$  value for a 95% probability [15]. The statistically significant contrasts are those whose absolute value is greater than zero with a probability of 95%. The analysis of results (Table 3) indicates, not only that one contrast out of three is noticeably significant ( $l_3$  for  $y_{Se}$ ,  $l_1$  for  $y_{Bi}$  and  $y_{Te}$ ), but also that the contrast  $l_2$  is not so significant. Therefore, it is possible to disregard the two-order interactions. The average at the centre of the design is comparable with the average of the four points of the  $2^{3-1}$  fractional factorial design and in this case the model equations obtained for each response are:

$$\hat{y} = average + \frac{l_1}{2}X_1 + \frac{l_2}{2}X_2 + \frac{l_3}{2}X_3$$

By examining the results it can be observed that for the  $\hat{y}_{Se}$  response all factors may be significant, hence:  $\hat{y}_{Se} = 0.235 + 0.044 X_1 + 0.023 X_2 + 0.126 X_3$ . Similarly the same factors for the  $\hat{y}_{Te}$  response are noted:  $\hat{y}_{Te} = 2.376 + 0.165 X_1 - 0.037 X_2 - 0.057 X_3$ . Regarding the  $\hat{y}_{Bi}$  response, it can be observed that the  $X_1$  and  $X_3$  factors have a significant influence:  $\hat{y}_{Bi} = 2.388 - 0.209 X_1 - 0.069 X_3$ . Considering the target value of each response, the optimum value of every factor is determined:  $X_1$  at a high level (+1),  $X_2$  at a low level (-1) and  $X_3$  at a high level (+1). So, the response of each model can be worked out:  $\hat{y}_{Bi} = 2.10$ ,  $\hat{y}_{Te} = 2.52$ ,  $\hat{y}_{Se} = 0.38$ .

Table 4. Comparison of observed  $d$ -values of thin film  $Bi_{1.97}(Te_{0.88}Se_{0.12})_{3.03}$  from XRD with ASTM standard  $d$ -values of  $Bi_2Te_3$  (set 15-863) and  $Bi_2Se_3$  (set 33-214) materials

ASTM $d$ values / $\text{\AA}$		h	k	l	$d$ values observed / $\text{\AA}$
$Bi_2Te_3$	$Bi_2Se_3$				
3.767	3.559	1	0	1	3.742
3.222	3.040	1	0	5	3.194
2.376	2.238	1	0	10	2.352
2.192	2.070	1	1	0	2.183
2.013	1.900	1	1	6	1.999
1.812	1.710	2	0	5	1.805
1.611	1.519	2	0	10	1.601
1.490	1.403	1	1	15	1.476
1.397	1.319	2	1	5	1.391
1.298	1.224	2	1	10	1.291
1.266	1.195	3	0	0	1.262

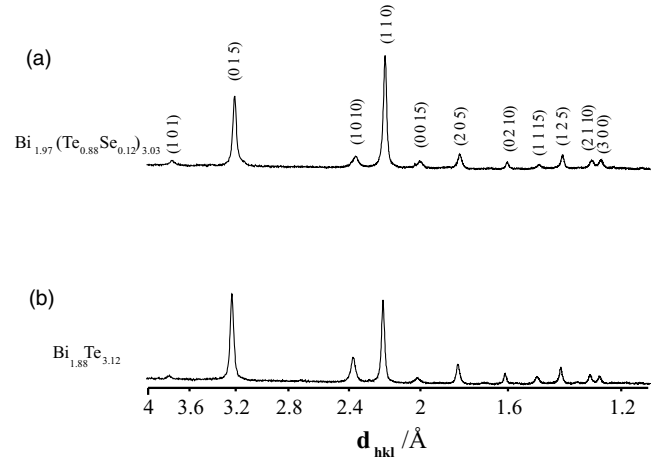


Fig. 2. X-ray diffraction diagrams of electrodeposited films obtained under potentiostatic conditions. (Radiation used:  $CoK_{\alpha}$ ;  $\lambda = 1.78897 \text{ \AA}$ ). (a)  $Bi_{1.97}(Te_{0.88}Se_{0.12})_{3.03}$  -  $E_{deposition} = -55 \text{ mV}$ , 60 at. % Bi - 36 at. % Te - 4 at. % Se in solution ( $10^{-2} \text{ M Bi}^{3+} + 6 \times 10^{-3} \text{ M HTeO}_2^+ + 6.65 \times 10^{-4} \text{ M Se}^{4+}$ ); b)  $Bi_2Te_3$  -  $E_{deposition} = -90 \text{ mV}$ , 50 at. % Bi - 50 at. % Te in solution ( $10^{-2} \text{ M Bi}^{3+} + 10^{-2} \text{ M HTeO}_2^+$ ).

As this run was not achieved, a deposition was carried out in these conditions ( $E_{deposition} = -55 \text{ mV}$ , an electrolyte composition fixed at 60 at. % Bi, 36 at. % Te and 4 at. % Se) during 2 h. The microprobe analysis of this run is in good agreement with the prediction but the film has a small excess of chalcogenide  $Bi_{1.97}Te_{2.67}Se_{0.36}$ .

### 3.3. Structural and microstructural analysis

The XRD patterns for the film deposited from the 60 at. % Bi-4 at. % Se-36 at. % Te solution and an electrodeposited  $Bi_2Te_3$  under potentiostatic polarization at  $E = -55 \text{ mV}$  and  $E = -90 \text{ mV}$  respectively, exhibit a single phase which has good crystallinity (Figure 2). The peaks were identified by comparing the  $d$ -values (Table 4) obtained from the XRD patterns with the American Standard for Testing and Materials (ASTM) data cards  $d$ -values. This alloy crystallizes with rhombohedral structure (R-3m) which is usually repre-

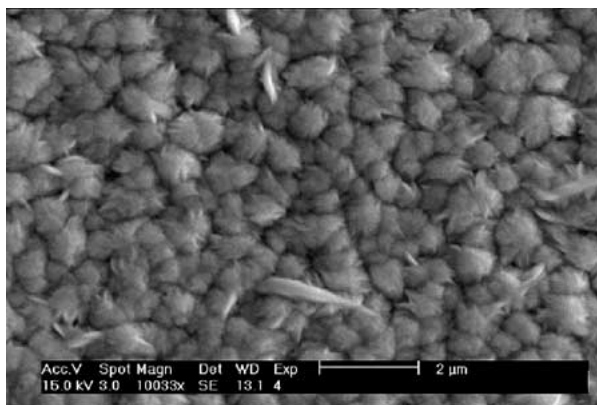


Fig. 3. SEM photograph of a  $\text{Bi}_{1.97}(\text{Te}_{0.88}\text{Se}_{0.12})_{3.03}$  film deposited onto stainless steel,  $E_{\text{deposition}} = -55$  mV, 60 at. % Bi, 36 at. % Te and 4 at. % Se in solution ( $10^{-2}$  M  $\text{Bi}^{3+}$  +  $6 \times 10^{-3}$  M  $\text{HTeO}_2^+$  +  $6.65 \times 10^{-4}$  M  $\text{Se}^{4+}$ ).

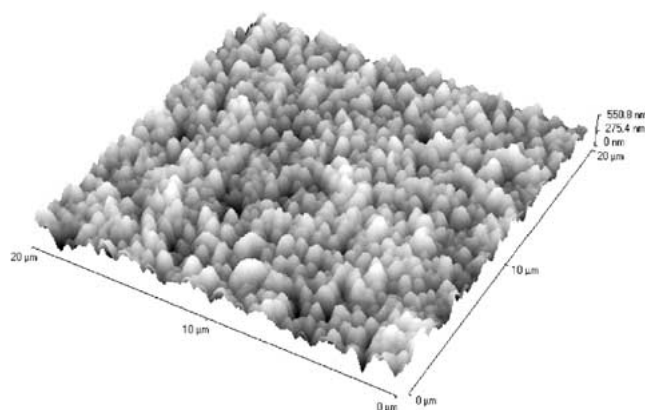


Fig. 4. AFM image of a  $\text{Bi}_{1.97}(\text{Te}_{0.88}\text{Se}_{0.12})_{3.03}$  film deposited onto stainless steel,  $E_{\text{deposition}} = -55$  mV, 60 at. % Bi, 36 at. % Te and 4 at. % Se in solution ( $10^{-2}$  M  $\text{Bi}^{3+}$  +  $6 \times 10^{-3}$  M  $\text{HTeO}_2^+$  +  $6.65 \times 10^{-4}$  M  $\text{Se}^{4+}$ ).

sented in the hexagonal lattice. The lattice parameters of the hexagonal structure were determined from the observed reticular distances, using a least-squares method. They are equal to  $a = 4.373$  (1) Å and  $c = 30.03$  (1) Å respectively.

The examination of an electrodeposited sample by SEM shows that the face in contact with the electrolyte is totally covered by crystallites which are agglomerated in roughly circular nodules with an average size of 1 μm (Figure 3). After removing the film, the face in contact with the support electrode exhibits a uniform surface with metallic lustre.

The surface smoothness of this film was further characterized by AFM. The advantage of AFM is its capacity to probe the minute details related to the individual grains. Figure 4 shows the three-dimensional representation of a  $20 \mu\text{m} \times 20 \mu\text{m}$  area of the electro-

deposited films; the RMS (root mean square) roughness is found to be 90 nm.

#### 4. Conclusion

An experimental design has been applied for the first time to the optimization of the electrodeposition process for ternary bismuth–tellurium–selenium alloys. These alloys were deposited by means of electrodeposition from aqueous solutions of  $\text{Bi}^{3+}$ ,  $\text{HTeO}_2^+$  and  $\text{Se}^{4+}$  in nitric acid. The linear voltammetry specifies the cathodic region where  $\text{Bi}_2(\text{Te}_{1-x}\text{Se}_x)_3$  can be deposited. By controlling the chemical and electrochemical parameters, it is possible to achieve a large range of composition of the ternary compounds. A protocol was defined leading to alloys with the best composition:  $\text{Bi}_{1.97}(\text{Te}_{0.88}\text{Se}_{0.12})_{3.03}$ . This sample is polycrystalline and exhibits a single phase. Further work will focus on the characterization of the semiconductive and thermoelectric properties of  $\text{Bi}_{1.97}(\text{Te}_{0.88}\text{Se}_{0.12})_{3.03}$  films.

#### References

1. T. Ohta, T. Kajikawa and Y. Kumashiro, *Electr. Eng. Jpn.* **110** (1990) 14.
2. J.H. Kiely and D.H. Lee, *Meas. Sci. Technol.* **8** (1997) 661.
3. S. Hava, H.B. Sequiera and R.G. Hunsperger, *J. Appl. Phys.* **58** (1985) 1727.
4. D.Y. Lou, *Appl. Opt.* **21** (1982) 1602.
5. A. Ioffe, 'Semiconductors Thermoelements and Thermoelectric Cooling'. Infosearch, London (1957).
6. B. Yim and F. Rosi, *Solid State Electronics* **15** (1957) 1121.
7. G. Hodes, S.J. Fonash, A. Heller and B. Miller, 'Advances Electrochemistry and Electrochemical Engineering' **13** (Wiley, New York, 1984), p. 113B.
8. C. De Mattei and R. Feigelson, 'Electrochemistry of Semiconductors and Electronics: Processes and Devices' (Noyes Publication, Park Ridge, New Jersey, USA, 1992).
9. M. Saitou, R. Yamaguchi and W. Oshikawa, *Mater. Chem. Phys.* **73** (2002) 306.
10. M. Takahashi, Y. Katou, K. Nagata and S. Furuta, *Thin Solid Films* **70** (1994) 240.
11. P. Magri, C. Boulanger and J.M. Lecuire, in Mathisprakasam and P. Heenan, (Eds), Proceeding 13th International Conference on 'Thermoelectricity', Kansas, (AIP Press, New York, 1995), p. 277.
12. P. Magri, C. Boulanger and J.M. Lecuire, *J. Mater. Chem.* **6** (1996) 773.
13. Y. Miyazaki and T. Kajitani, *J. Crystal Growth* **229** (2001) 542.
14. J.P. Fleuriel, A. Borsheevsky, M.A. Ryan, W.M. Phillips, J.G. Snyder, T. Caillat, E.A. Kolawa, J.A. Herman, P. Mueller and M. Nicolet, *Mater. Res. Soc.* **545** (1999) 493.
15. J. Goupy, 'Methods for Experimental Design' (Elsevier, Amsterdam 1993).
16. J.C. Miller and J.N. Miller, Statistics for Analytical Chemistry (Ellis Harwood and Prentice Hall, Englewood Cliffs, NJ, 1994).
17. S. Pinzauti, P. Gratteri, S. Furlanetto, P. Mura, E. Dreassi and R. Phan-Tan-Luu, *J. Pharm. Biomed. Analysis* **41** (1996) 881.
18. K.D. Altria and S.D. Filbey, *Chromatographia* **39** (1994) 306.
19. G.E.P. Box, X.G. Hunter and J.S. Hunter, 'Statistics for Experimenters' (Wiley, New York, 1978).